

# Molecular Dynamics Study of a Hexadecyltrimethylammonium Chloride Monolayer at the Interface between Two Immiscible Liquids

Daniel J. V. A. dos Santos\* and José A. N. F. Gomes

CEQUP/Departamento de Química da Faculdade de Ciências da Universidade do Porto,  
R. Campo Alegre 687, 4069-007 Porto, Portugal

Received August 21, 2002. In Final Form: October 20, 2002

We have simulated a hexadecyltrimethylammonium (CTA) chloride monolayer adsorbed at the water/air and water/1,2-dichloroethane (DCE) interfaces. A diffusive electrical double layer was found formed by the chloride and CTA ions. It was found that the water molecules change their dipole orientation to help on the neutralization of this electrical charged layer. The DCE molecules penetrate the CTA tails and an increased concentration exists inside the tails. The tilt angle maximum probability for the CTA tails is 20° at the water/DCE interface, while at the water/air interface the maximum probability is located at 40°. The average tilt angle values are 27° and 40°, respectively. The average number of trans conformations per chain is similar at both interfaces with a maximum probability corresponding to 12 trans conformations. Nevertheless, the percentage of trans conformations in the chains is greater for the water/DCE interface and consequently the CTA tails at the water/air interface are more folded, present more defects, and are less stretched. The distribution of the chains is broader when the monolayer is adsorbed at the water/DCE interface. The motion in the monolayer plane of the terminal methyl group is less at the water/DCE interface.

## 1. Introduction

Molecular monolayers and thin films have been extensively studied for more than a century. They display complex phase diagrams and elaborate structures<sup>1</sup> and pose some yet unresolved chemical problems. They play an important role in processes such as lubrication, molecule self-assembly, foam stability, ion transfer, microemulsions, and detergency. They are extensively used in several industries, such as the mining and oil industry for extraction and separation or the household industry for fabric softeners.<sup>2</sup>

The appearance of several review articles concerning the chemistry of organized surfactant systems<sup>2–7</sup> and the development of instrumentation and analysis techniques<sup>8</sup> are a clear indication of the extensive research carried out in this field of chemistry.

The study of monolayer systems can be very valuable since they are simplified models for bilayers or biological membranes. For this reason, the detailed study of the electrostatic potential profile and the dielectric profile is very important if we want to evolve to a good mesoscale description of monolayers and bilayers adsorbed between two immiscible liquids or the interactions of druglike molecules with adsorbed films.

The theoretical treatment of this kind of system began by the use of lattice models or the application of mean

field theory approximation. The early simulations accounted for the main features using idealized oil-like and waterlike particles and the surfactant being a mixture of both particles.<sup>9,10</sup>

A large number of computational and theoretical studies<sup>11–13</sup> have been done in monolayers and bilayers of Langmuir and Langmuir–Blodgett interfaces since the pioneering computational studies by Smit<sup>14</sup> and Berendsen et al.<sup>15,16</sup> Yet only a small number of computational investigations have been carried out at the interface between two immiscible liquids.<sup>17–20</sup>

Monolayers between two immiscible liquids are suitable for studies by electrochemistry techniques, namely, cyclic voltammetry. They are easily built and mechanically stable, and the potential drop across the interface can be accurately controlled externally.<sup>21–24</sup>

\* To whom correspondence should be addressed. E-mail: dasantos@fc.up.pt.

(1) Wu, P.; Zeng, Q.; Xu, S.; Wang, C.; Yin, S.; Bai, C.-L. *ChemPhysChem* **2002**, *2*, 750.

(2) Swalen, J. D.; Allara, D. L.; Andrade, J. D.; Chandross, E. A.; Garoff, S.; Israelachvili, J.; McCarthy, T. J.; Murray, R.; Pease, R. F.; Rabolt, J. F.; Wynne, K. J.; Yu, H. *Langmuir* **1987**, *3*, 932.

(3) Shinoda, K.; Lindman, B. *Langmuir* **1987**, *3*, 135.

(4) Whitesides, G. M.; Laibinis, P. E. *Langmuir* **1990**, *6*, 87.

(5) Gelbart, W. M.; Ben-Shaul, A. *J. Phys. Chem.* **1996**, *100*, 13169.

(6) Miranda, P. B.; Shen, Y. R. *J. Phys. Chem. B* **1999**, *103*, 3292.

(7) Lu, J. R.; Thomas, R. K.; Penfold, J. *Adv. Colloid Interface Sci.* **2000**, *84*, 143.

(8) Penfold, J. *Curr. Opin. Colloid Interface Sci.* **2002**, *7*, 139.

(9) Smit, B.; Hilberts, P. A. J.; Esselink, K.; Rupert, L. A. M.; van Os, N. M.; Schlijper, A. G. *Nature* **1990**, *348*, 624.

(10) Smit, B.; Hilberts, P. A. J.; Esselink, K.; Rupert, L. A. M.; van Os, N. M.; Schlijper, A. G. *J. Phys. Chem.* **1991**, *95*, 6361.

(11) da Gama, M. M. T.; Gubbins, K. E. *Mol. Phys.* **1986**, *59*, 227.

(12) Rieu, J. P.; Vallade, M. *J. Chem. Phys.* **1996**, *104*, 7729.

(13) Vincze, A.; Horvai, G.; Leermakers, F. A. M. *Electrochim. Acta* **1995**, *40*, 2875.

(14) Smit, B. *Phys. Rev. A* **1988**, *37*, 3431.

(15) van der Ploeg, P.; Berendsen, H. J. C. *J. Chem. Phys.* **1982**, *76*, 3271.

(16) Egberts, E.; Berendsen, H. J. C. *J. Chem. Phys.* **1988**, *89*, 3718.

(17) Schweighofer, K. J.; Essmann, U.; Berkowitz, M. *J. Phys. Chem. B* **1997**, *101*, 3793.

(18) Schweighofer, K. J.; Essmann, U.; Berkowitz, M. *J. Phys. Chem. B* **1997**, *101*, 10775.

(19) Dominguez, H.; Smondyrev, A. M.; Berkowitz, M. L. *J. Phys. Chem. B* **1999**, *103*, 9582.

(20) Dominguez, H.; Berkowitz, M. L. *J. Phys. Chem. B* **2000**, *104*, 5302.

(21) Wandlowski, T.; Mareček, V.; Samec, Z. *J. Electroanal. Chem.* **1988**, *242*, 277.

(22) Cunnane, V. J.; Schiffrin, D. J.; Fleischmann, M.; Goblewicz, G.; Williams, D. *J. Electroanal. Chem.* **1988**, *243*, 455.

(23) Kakiuchi, T.; Nakanishi, M.; Senda, M. *Bull. Chem. Soc. Jpn.* **1989**, *62*, 403.

(24) Kakiuchi, T.; Kondo, T.; Kotani, M.; Senda, M. *Langmuir* **1992**, *8*, 169.

Some experimental techniques used to study thin films, such as Brewster angle microscopy,<sup>25</sup> Fourier transform infrared spectroscopy,<sup>26</sup> or optical sum-frequency generation,<sup>27,28</sup> among others, although important, are unable to give detailed information at a molecular level. Meanwhile, the molecular information obtained by atomistic computer simulations can now be compared with experimental data from new techniques such as vibrational sum frequency generation spectroscopy,<sup>29,30</sup> neutron reflection,<sup>31–35</sup> or scanning tunneling microscopy.<sup>1,36</sup> Nevertheless, these techniques have been mainly applied to the water/air interface.

The molecular behavior of a monolayer between two immiscible liquids is very difficult to observe directly, even by the newest experimental techniques. Only recently Conboy et al.<sup>37</sup> have applied vibrational sum-frequency spectroscopy to a series of monolayers adsorbed at the deuterated water and carbon tetrachloride interface and Penfold<sup>38,39</sup> and co-workers have studied a monolayer of monododecyl pentaethylene glycol at the solution/air interface with and without an oil layer of dodecane and dodecyl and hexadecyltrimethylammonium bromide monolayers mixed with dodecane at the water/air interface.

The molecular dynamics simulation method has given insightful information when applied to the study of the interface between two immiscible liquids<sup>40–45</sup> or to the ion transfer across this interface type.<sup>46–54</sup> In this work, we study the behavior of a hexadecyltrimethylammonium chloride monolayer adsorbed at the interface between

water/air and water/1,2-dichloroethane (DCE) by molecular dynamics.

Böcker<sup>55</sup> and co-workers have simulated the behavior of a hexadecyltrimethylammonium chloride (CTAC) monolayer at the water/air interface with an area per headgroup of 45 Å<sup>2</sup>. They studied two systems, one containing 32 CTACs and another containing 64 CTACs. They present mainly the results for the bigger system and find, for this system, a wavelike arrangement of the headgroups that is absent in the smaller one. They conclude that the system size has an effect on the calculated properties. This observation is in accordance with earlier observations<sup>56–58</sup> of the severe influence of the system size on the properties of monolayers.

The influence of the monolayer size upon the properties of the system depends on the surface coverage density, the length and nature of the surfactant tails (branched, functionalized), the nature and charge of the heads, the tilt angle distribution, and the type of interface in which the surfactant is adsorbed. As far as we know, little work has been done to understand this important phenomenon, and some results appear to be contradictory. In fact, Bishop and Clarke<sup>56</sup> simulated a Langmuir–Blodgett monolayer with 16, 64, and 100 surfactant molecules and concluded that for the densities used (19.6, 20.8, 22.0, and 23.2 Å<sup>2</sup> per chain) a 64 chain system was large enough to give accurate calculations of the tilt angle. Siepmann and McDonald<sup>57</sup> simulated three different Langmuir–Blodgett monolayers with 30, 90, and 224 chains at 21 Å<sup>2</sup> per chain. They find a difference in the degree of homogeneity with the smaller systems formed by a single domain. For the larger system, they also found that the domain boundaries were clearly visible and the surfactants presented a different tilt angle and larger than average conformational defects. Due to the higher disorder, the mean potential energy was higher for the larger system and the thickness of the monolayer was weakly dependent on the system size. For the radial distribution functions, they find a broadening of the peaks but no shifting. Karaborni and Siepmann<sup>58</sup> find a lower level of ordering in a 256 than on a 64 surfactant system.

Klein and co-workers<sup>59</sup> have also studied a similar system containing 64 tetradecyltrimethylammonium bromide (CTAB) molecules at two different areas per headgroup (45 and 67 Å<sup>2</sup>) built on opposite sides of a water lamella (32 CTABs on each monolayer of both sides).

In a previous attempt to build our system, a simple test with a monolayer containing 36 CTACs demonstrated that the collective properties of the monolayer corresponded clearly to a more ordered system. Indeed, this effect due to the periodic boundary conditions on systems containing monolayers with small box sizes was already noticed, and the effect of the box side length is even more pronounced in this kind of system where the surfactant has a net charge.

Not only the monolayer size is important, but also the lamella of neighboring liquids used. The counterions that are dissolved on the water lamella should not feel the presence of some kind of interface that may exist on the water side but only feel the presence of bulk water. Since the major contribution to the total number of sites is by far coming from the ones present on the liquid lamellae,

- (25) Hönig, D.; Möbius, D. *J. Phys. Chem.* **1991**, *95*, 4590.  
 (26) Du, X.; Shi, B.; Liang, Y. *Langmuir* **1998**, *14*, 3631.  
 (27) Hunt, J. H.; Guyot-Sionnest, P.; Shen, Y. R. *Chem. Phys. Lett.* **1987**, *133*, 189.  
 (28) Miranda, P. B.; Pflumio, V.; Saijo, H.; Shen, Y. R. *Chem. Phys. Lett.* **1997**, *264*, 387.  
 (29) Bell, G. R.; Bain, C. D.; Li, Z. X.; Thomas, R. K.; Duffy, D. C.; Penfold, J. *J. Am. Chem. Soc.* **1997**, *119*, 10227.  
 (30) Bell, G. R.; Manning-Benson, S.; Bain, C. D. *J. Phys. Chem. B* **1998**, *102*, 218.  
 (31) Simister, E. A.; Lee, E. M.; Thomas, R. K.; Penfold, J. *J. Phys. Chem.* **1992**, *96*, 1373.  
 (32) Lu, J. R.; Hromadova, M.; Simister, E. A.; Thomas, R. K.; Penfold, J. *J. Phys. Chem.* **1994**, *98*, 11519.  
 (33) Lu, J. R.; Li, Z. X.; Smallwood, J.; Thomas, R. K.; Penfold, J. *J. Phys. Chem.* **1995**, *99*, 8233.  
 (34) Lu, J. R.; Li, Z. X.; Thomas, R. K.; Penfold, J. *J. Chem. Soc., Faraday Trans.* **1996**, *92*, 403.  
 (35) Lu, J. R.; Thomas, R. K. *J. Chem. Soc., Faraday Trans.* **1998**, *94*, 995.  
 (36) Xu, S.-L.; Wang, C.; Zeng, Q.-D.; Wu, P.; Wang, Z.-G.; Yan, H.-K.; Bai, C.-L. *Langmuir* **2002**, *18*, 657.  
 (37) Conboy, J. C.; Messner, M. C.; Richmond, G. L. *J. Phys. Chem.* **1997**, *101*, 6724.  
 (38) Lu, J. R.; Thomas, R. K.; Binks, B. P.; Fletcher, P. D. I.; Penfold, J. *J. Phys. Chem.* **1995**, *99*, 4113.  
 (39) Lu, J. R.; Li, Z. X.; Thomas, R. K.; Binks, B. P.; Crichton, D.; Fletcher, P. D. I.; McNab, J. R.; Penfold, J. *J. Phys. Chem. B* **1998**, *102*, 5785.  
 (40) Lynse, P. *J. Chem. Phys.* **1987**, *86*, 4177.  
 (41) Benjamin, I. *J. Chem. Phys.* **1992**, *97*, 1432.  
 (42) Pohorille, A.; Wilson, M. A. *THEOCHEM* **1993**, *284*, 271.  
 (43) Benjamin, I. *Chem. Rev.* **1996**, *96*, 1449.  
 (44) Michael, D.; Benjamin, I. *J. Electroanal. Chem.* **1998**, *450*, 335.  
 (45) Fernandes, P. A.; Cordeiro, M. N. D. S.; Gomes, J. A. N. F. *J. Phys. Chem. B* **1999**, *103*, 6290.  
 (46) Benjamin, I. *J. Chem. Phys.* **1992**, *96*, 577.  
 (47) Benjamin, I. *Science* **1993**, *261*, 1558.  
 (48) Benjamin, I. *Chem. Phys.* **1994**, *180*, 287.  
 (49) Schweighofer, K. J.; Benjamin, I. *J. Phys. Chem.* **1995**, *99*, 9974.  
 (50) Benjamin, I. Molecular Dynamics of charge transfer at the liquid/liquid interface. In *Liquid–liquid interfaces: Theory and methods*; Volkov, A. G., Deamer, D. W., Eds.; CRC Press: Boca Raton, FL, 1996.  
 (51) Chang, T.-M.; Dang, L. X. *J. Chem. Phys.* **1998**, *108*, 818.  
 (52) Schweighofer, K.; Benjamin, I. *J. Phys. Chem. A* **1999**, *103*, 10274.  
 (53) Fernandes, P. A.; Cordeiro, M. N. D. S.; Gomes, J. A. N. F. *J. Phys. Chem. B* **1999**, *103*, 8930.  
 (54) Fernandes, P. A.; Cordeiro, M. N. D. S.; Gomes, J. A. N. F. *J. Phys. Chem. B* **2000**, *104*, 2278.

- (55) Böcker, J.; Schlenkrich, M.; Bopp, P.; Brickmann, J. *J. Phys. Chem.* **1992**, *96*, 9915.  
 (56) Bishop, M.; Clarke, J. H. R. *J. Chem. Phys.* **1991**, *95*, 540.  
 (57) Siepmann, J. I.; McDonald, I. R. *Langmuir* **1993**, *9*, 2351.  
 (58) Karaborni, S.; Siepmann, J. I. *Mol. Phys.* **1994**, *83*, 345.  
 (59) Tarek, M.; Tobias, D. J.; Klein, M. L. *J. Phys. Chem.* **1995**, *99*, 1393.

their increase poses a problem because the computation time is proportional to the square of the number of sites.

As the natural state of the biological membranes is liquidlike, the molecular study of monolayers at a similar state can bring valuable information about the possible relations between structure, behavior, and kinetics of interfacial processes.

As most theoretical studies are performed at the water/air interface and experimental electrochemistry is performed at liquid/liquid interfaces, the main purpose of this article is to understand at the microscopic level what are the differences in structure and behavior of monolayers when a bulk oil layer is added and a liquid/liquid interface is constructed. We want to understand how properties are changed in order to use the large amount of information gathered at the water/air interface for the interpretation of phenomena at liquid/liquid interfaces. On the other hand, there is some information at the molecular level that despite the advances in the experimental techniques still is not yet accessible but can be obtained by this type of computer simulation.

## 2. Simulation Details

For the water potential, we used the simple point charge model (SPC model<sup>60</sup>). For the hexadecyltrimethylammonium ion, we used the charges calculated by Böcker and co-workers<sup>55</sup> with the van der Waals and ligand forces parametrization of the CHARMM22<sup>61</sup> force field except for the dihedral angle that was replaced by the Ryckaert–Bellemans<sup>62,63</sup> description. For the DCE, we used the potential developed by Jorgensen and co-workers.<sup>64</sup> For the chloride ion, we use the parameters developed by Smith and Dang.<sup>65</sup>

The water angle and all bond lengths were constrained using the SHAKE<sup>66</sup> algorithm with a tolerance of  $10^{-5}$  Å.

To obtain the Lennard-Jones parameters between sites of unlike atoms, the Lorentz–Berthelot<sup>61,67</sup> mixing rule was used (as required by the CHARMM22 potential).

All simulations were performed with a modified version of the DL\_POLY<sup>68</sup> molecular dynamics package in the NAT ensemble ( $T = 300$  K) using a Nosé–Hoover<sup>69,70</sup> thermostat in the Melchionna et al.<sup>71</sup> implementation.

Periodic boundary conditions were applied in the monolayer surface ( $x$  and  $y$  axes) except for the longitudinal axis in which the system interfaced with a vacuum.

In all the simulations, the velocity Verlet algorithm was used for the integration of the equations of motion with a time step of 2 fs. A 10 Å cutoff was used for the short-range interactions and a 12 Å one for the long-range

interactions with a smoothing function<sup>72</sup> applied between 11 and 12 Å. A multiple time step was also used for interactions greater than 11.5 Å with an update frequency of 8 time steps. A system check in the microcanonical ensemble was performed to verify the validity of the parameters, and a good energy conservation was found.

The system was prepared by constructing a square lattice monolayer with 100 hexadecyltrimethylammonium ions with 45 Å<sup>2</sup> per headgroup. This corresponds to a cross section of about  $67 \times 67$  Å<sup>2</sup>. All the hexadecyltrimethylammonium tail dihedral angles were set in a trans conformation and parallel to the  $z$  axis. Chloride ions were added at a distance of about 3–4 Å from the hexadecyltrimethylammonium head positions. A rapid equilibration was performed with the nitrogen atom positions frozen just to randomize the tails, changing the orientation and the dihedral conformations. In all the following simulations, the nitrogen atom positions were free to move according to Newtonian dynamics.

A water box with 4500 molecules and a box containing 1372 DCE molecules, with the same cross section of about  $50 \times 50$  Å<sup>2</sup>, were equilibrated for 150 ps in the  $NpT$  ensemble with periodic boundary conditions and simulation parameters similar to those described for the hexadecyltrimethylammonium chloride lattice.

The water molecules split across the boundaries were reunited and a system corresponding to a Langmuir interface was constructed by joining together the hexadecyltrimethylammonium chloride layer and the water box with a gap of 3–4 Å between them. A new equilibration of 300 ps was performed in the NAT ensemble with periodic boundary conditions in all axes except the longitudinal  $z$  axis. The molecules of the DCE box which were split across the boundaries were joined together. Finally, the monolayer between water and DCE was constructed by joining the oil box to the Langmuir interface using a gap of 3–4 Å between the hexadecyltrimethylammonium tails and the oil molecules. This system has about 100 Å along the major  $z$  axis. The systems interface with a vacuum at both ends of the longitudinal  $z$  axis and have periodic boundary conditions in the monolayer plane ( $x$  and  $y$  axes). In this way, we have obtained two systems with monolayers adsorbed at the water/air and water/DCE interfaces with exactly the same coverage density (45 Å<sup>2</sup> per headgroup).

Both systems were equilibrated for at least 1200 ps. After this equilibration, a production run was started for 1000 ps. During this production run, the trajectories of the particles present in the systems were written to files every 32 steps and later analyzed.

The use of Ewald summations or the effect of truncations on the properties of the systems under study has been discussed in the literature. For systems containing charges, the interactions are more accurately calculated by Ewald summations, but only recently an efficient and accurate way was developed to perform these calculations on systems containing periodicity in two dimensions.<sup>73</sup> As the system size affects the calculated properties, a compromise is needed between system size and computation time. We opted for the use of truncation with a smoothing function<sup>72</sup> as we believe that the effect of this kind of approximation is less severe than the use of a small number of surfactant molecules.

(60) Berendsen, H. J.; Postma, J. P. M.; van Gunsteren, W. F.; Hermans, J. In *Intermolecular Forces*; Pullman, B., Ed.; Reidel: Dordrecht, The Netherlands, 1981.

(61) MacKerell, A. D., Jr.; et al. *J. Phys. Chem. B* **1998**, *102*, 3586.

(62) Ryckaert, J.-P.; Bellemans, A. *Chem. Phys. Lett.* **1975**, *30*, 123.

(63) Ryckaert, J.-P.; Bellemans, A. *Faraday Discuss. Chem. Soc.* **1978**, *66*, 95.

(64) Jorgensen, W. L.; McDonald, N. A.; Selmi, M.; Rablen, P. R. *J. Am. Chem. Soc.* **1995**, *117*, 11809.

(65) Smith, D. E.; Dang, L. X. *J. Chem. Phys.* **1994**, *100*, 3757.

(66) Ryckaert, J.-P.; Cicciotti, G.; Berendsen, H. J. C. *J. Comput. Phys.* **1977**, *23*, 327.

(67) Allen, M. P.; Tildesley, D. J. *Computer Simulation of Liquids*; Oxford University Press: Oxford, 1990.

(68) Forrester, D. W.; Smith, W. *DL\_POLY*, version 2.11; CCLRC Daresbury Laboratory: Daresbury, U.K., 1998.

(69) Nosé, S. Molecular dynamics simulations at constant temperature and pressure. In *Computer Simulation in Materials Science*; Meyer, M., Pontikis, V., Eds.; Kluwer Academic Publishers: Netherlands, 1991.

(70) Hoover, W. G. *Phys. Rev. A* **1985**, *31*, 1695.

(71) Melchionna, S.; Cicciotti, G.; Holian, B. L. *Mol. Phys.* **1993**, *78*, 533.

(72) Brooks, C. L., III; Pettitt, B. M.; Karplus, M. *J. Chem. Phys.* **1985**, *83*, 5897.

(73) Minary, P.; Tuckerman, M. E.; Pihakari, K. A.; Martyna, G. J. *J. Chem. Phys.* **2002**, *116*, 5351.



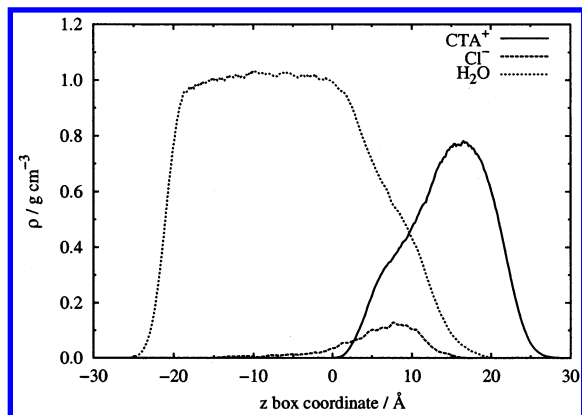


**Figure 1.** Average density profiles for the water, chloride ions, and CTA ions as a function of the box coordinate for the Langmuir interface (water/air).

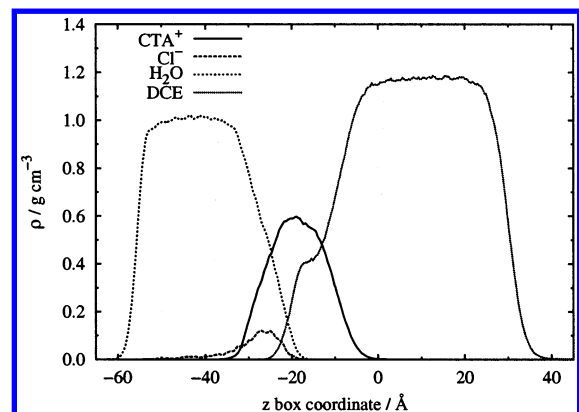


**Figure 2.** Average density profile for the water, chloride ions, CTA ions, and DCE as a function of the box coordinate for the water/DCE interface.

### 3. Results

The systems simulated are represented in Figure 1 by the density profile of the CTA monolayer adsorbed at the water/air interface and in Figure 2 by the average density profile of the monolayer adsorbed at the water/DCE interface. As can be seen in these figures, the density profiles match the bulk densities of the liquids.

Figures 1 and 2 show a diffuse electrical double layer formed by a negatively charged diffuse barrier of chloride ions and a positively charged diffuse barrier of CTA heads. The penetration of the water molecules stops at the point where there are no more heads to be solvated. The diffusive layer of chloride ions is located mainly near the CTA heads, but some of the ions diffuse throughout the water lamella.

It is important to note in Figure 2 that the density profile of the DCE lamella near the CTA tails and the density profile of the water near the CTA heads are rather different. While the water profile decreases almost linearly, the DCE profile has a little shoulder that indicates a greater DCE concentration. It seems that the DCE molecules are concentrated to a greater extent in the region where they start to feel the presence of the double layer charges already inside the CTA chains. The penetration of oil-like molecules in monolayers was experimentally observed for dodecane on tetradecyltrimethylammonium bromide<sup>74</sup> and dodecyl and hexadecyltrimethylammonium bromide<sup>38</sup> monolayers and other monolayers.<sup>39</sup>

(74) Lu, J. R.; Thomas, R. K.; Aveyard, R.; Binks, B. P.; Cooper, P.; Fletcher, P. D. I.; Sokolowski, A.; Penfold, J. *J. Phys. Chem.* **1992**, *96*, 10971.

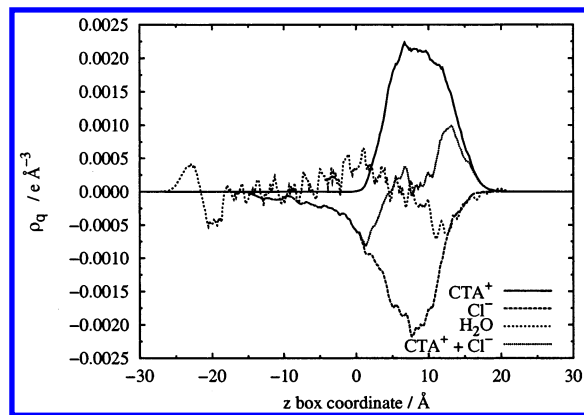


**Figure 3.** Average electron density profile for the water, chloride ions, CTA ions, and CTA plus chloride as a function of the box coordinate for the water/air interface.

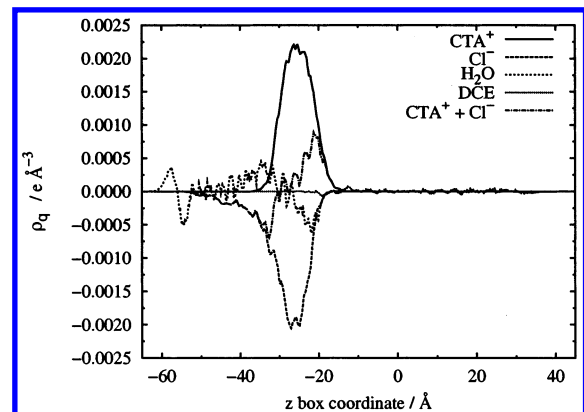


**Figure 4.** Average electron density profile for the water, chloride ions, CTA ions, and CTA plus chloride as a function of the box coordinate for the water/DCE interface.

The density maximum of the CTA is greater when adsorbed at the water/air interface than when adsorbed at the water/DCE interface. This indicates that the CTA ions are more folded when adsorbed at the water/air interface since there is nothing to interact with. The chloride counterions are mainly located near the CTA charged headgroups and exist only in the water side (they do not cross the CTA tails).

The average electron density profiles for the CTA ions adsorbed at the water/air interface and at the water/DCE interface are represented in Figures 3 and 4, respectively. The counterions do not have the ability to completely neutralize the positive charge layer formed by the CTA headgroups, and the orientation of the water molecule dipoles is important. This behavior occurs at both interfaces, and the contribution of the water molecules is different near the headgroups from that near the tails since the average electron density profile for the sum of the CTA and chloride ions changes sign.

In Figures 5 and 6, the number density profiles for the water and CTA heads and tails are presented. The fits to the water profiles were done using the same hyperbolic tangent function that is commonly used by the experimentalists:<sup>7</sup>

$$\rho = \frac{\rho_0}{2} \left[ 1 \pm \tanh\left(\frac{z - z_0}{\xi}\right) \right] \quad (1)$$

where  $\xi$  is the width of the distribution and  $z_0$  is the center.

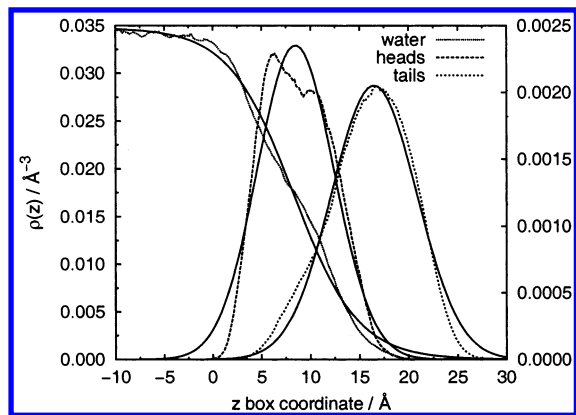


**Figure 5.** Profiles for the water and CTA (heads and tails) number densities at the Langmuir interface. The fits are also displayed. The water scale is on the left-hand side.

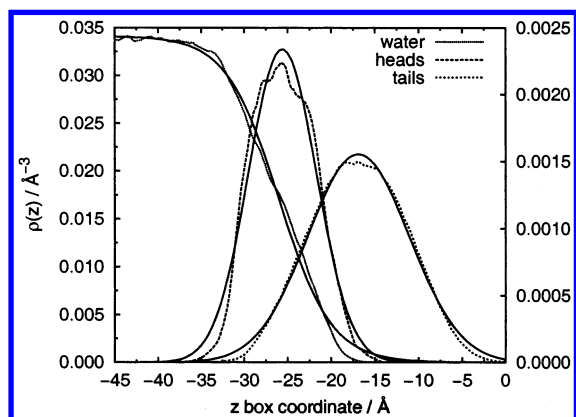


**Figure 6.** Profiles for the water and CTA (heads and tails) number densities at the water/DCE interface. The fits are also displayed. The water scale is on the left-hand side.

For the CTA heads and tails, a Gaussian function was used:

$$\rho = \rho_0 \exp\left[-4\left(\frac{(z - z_0)^2}{\sigma^2}\right)\right] \quad (2)$$

where  $\sigma$  is the width of the distribution and  $z_0$  is also the center.

The parameters obtained by fitting the simulation results are presented in Table 1.

In analysis of the values in Table 1, it should be noticed that due to the added contribution of the thermal roughness, the experimental value for  $\sigma_c$  should be corrected:

$$\sigma_{\text{obs}}^2 = \sigma_{\text{cor}}^2 + w \quad (3)$$

where obs means observed value and cor means corrected value.

The corrected  $\sigma_c$  obtained by Lu et al.<sup>7</sup> is 10 for the hexadecyltrimethylammonium which is much closer to the value that we have obtained. We should also be careful when comparing these values with the results obtained by Tarek et al.<sup>59</sup> because of the different definition for  $\sigma$ . We have used the experimental definition for the width, while they have used the full width at half-maximum (they differ by a factor of  $(\ln 2)^{1/2}$ ). Nevertheless, these results are in fair agreement with the results obtained by Tarek et al. for a tetradecyltrimethylammonium bromide monolayer. The larger values are due to the fact that the surfactant that we have used as a longer chain.

If we compare the behavior of the CTA in the two interfaces, we find that  $\sigma_h$  has the same value. On the other hand, the width for the distribution of the chains is larger for the water/DCE interface. The larger values for the distances between the distribution centers occur also at the water/DCE interface. This means that the CTA tails must have a greater percentage of trans conformations or must be more aligned with the interface normal. This will be analyzed later in more detail, and we will see that both of these contributions are positive.

The tilt angle  $\theta$  is defined as

$$\theta = \arccos\left(\frac{\mathbf{Z} \cdot \mathbf{R}_{\text{IN}}}{|\mathbf{R}_{\text{IN}}|}\right) \quad (4)$$

where  $\mathbf{R}_{\text{IN}}$  is the vector between the nitrogen atom and the terminal methyl group in the same molecule,  $\mathbf{R}_1 - \mathbf{R}_N$ , and  $\mathbf{Z}$  is the unit vector of the  $z$  axis. This angle was calculated over all the CTA ions, and a probability distribution was obtained for both interfaces. As can be seen in Figure 7, the presence of the DCE liquid phase changes the tilt angle distribution. For the CTAs adsorbed at the water/air interface, the average angle and the maximum probability are located around  $40^\circ$  (average,  $40 \pm 19$ ). A different behavior is observed for the CTAs adsorbed at the water/DCE interface. The maximum probability for this interface is located at near  $20^\circ$ , and the profile is much sharper (average,  $27 \pm 15$ ). In this case, a greater difference between the average tilt angle and the maximum probability exists because this distribution is less symmetric. This dramatic difference should be experimentally observed with appropriate techniques and can certainly cause differences in some interfacial phenomena such as the interactions of druglike molecules with monolayers.

For both interfaces, the existence of a tail in the tilt angle distribution means that some CTA ions prefer large angle values. Nevertheless, for the water/DCE interface there are no CTA ions parallel to the interface, unlike the CTA ions at the water/air interface.

A similar mean tilt angle value was obtained by Böcker et al., but the tilt angle distribution is a little broader with a maximum probability near  $20^\circ$ . This difference is possibly due to the system size dependence and also to a short production run (100 ps) as we could notice that the maximum probability does not have a rapid statistical convergence.

Comparing Figures 8 and 9, we find a great similarity between the tilt angle distribution for the CTA ions at the Langmuir interface that have a greater penetration in the water and the average distribution for the water/DCE interface. This means that these CTA ions feel the presence of the remainder of the surfactant layer as an added oil layer. This result is interesting and means that the data gathered for monolayers with an added oil layer, obtained from neutron reflection experiments,<sup>38,39,74</sup> could be used to help in more directly understanding the behavior of monolayers at liquid/liquid interfaces.

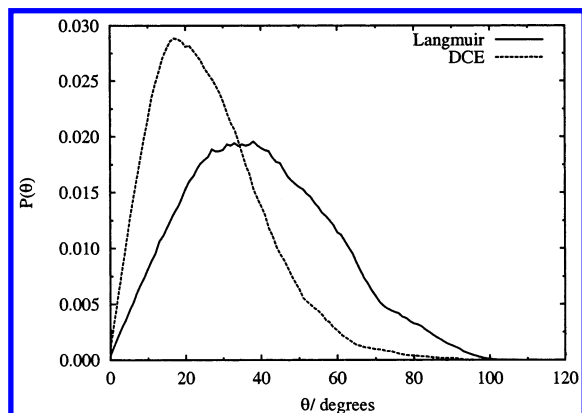
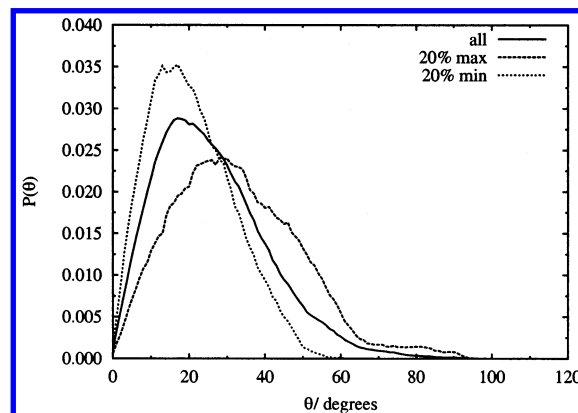
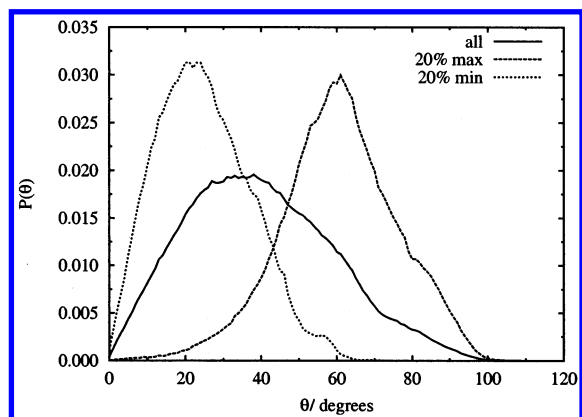
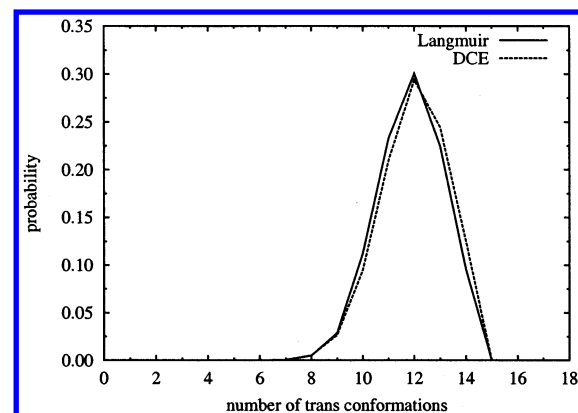
We can also see the greater disorder of the chains at the Langmuir interface when compared with the water/DCE interface.

The average number of trans conformations per chain at both interfaces is similar, with a maximum probability corresponding to 12 trans conformations (cf. Figure 10). This corresponds to the preference of 2 gauche conformations per chain and is in good agreement with the results of Böcker et al. Nevertheless, in the water/DCE interface, the CTA chains have a little less defects. This is under-

**Table 1. Widths  $\zeta$  and  $\sigma$  of the Water and CTA Head and Tail Profiles As Defined by Equations 1 and 2<sup>a</sup>**

interface	$\sigma_w/\text{\AA}$	$\sigma_c/\text{\AA}$	$\zeta/\text{\AA}$	$\delta_{ch}/\text{\AA}$	$\delta_{hs}/\text{\AA}$	$\delta_{cs}/\text{\AA}$
Langmuir, this work	$11.0 \pm 0.2$	$12.3 \pm 0.1$	$6.53 \pm 0.09$	$8.0 \pm 0.1$	$0.2 \pm 0.1$	$8.22 \pm 0.09$
Langmuir, expt	$14 \pm 3$	$16.5 \pm 1$	$6.5 \pm 1$	$8.0 \pm 0.5$	$2 \pm 1.5$	$9.0 \pm 0.5$
water/DCE, this work	$11.0 \pm 0.1$	$16.45 \pm 0.07$	$5.97 \pm 0.08$	$8.72 \pm 0.06$	$0.40 \pm 0.09$	$9.12 \pm 0.08$

<sup>a</sup>  $\delta_{ij}$  are the separations between the distribution centers (c, chains; h, heads; s, water). The experimental values were taken from Lu et al. (ref 7), uncorrected (see eq 3).

**Figure 7.** Tilt angle distribution of the CTA ions for the Langmuir interface and for the water/DCE interface.**Figure 9.** Probability to find a given number of trans conformations in the CTA chain for the water/DCE interface. The 20% max/min refers to the 20% of CTA ions that have the nitrogen atom with a larger/smaller  $z$  position (less/more penetration in the layer).**Figure 8.** Probability to find a given number of trans conformations in the CTA chain for the Langmuir interface. The 20% max/min refers to the 20% of CTA ions that have the nitrogen atom with a larger/smaller  $z$  position (less/more penetration in the layer).**Figure 10.** Probability of finding a given number of trans conformations in the CTA chain.

standable, since the presence of another condensed phase stabilizes energetically the trans conformations.

The influence of the DCE oil phase on the CTA tail bond conformations is more clearly seen if we report the percentage of trans conformations per bond number (cf. Figure 11).

When we go through the CTA chain from the water into the oil phase, the number of trans conformations diminishes at both interfaces. The terminal dihedral has also the greater percentage of gauche conformations at both interfaces. However, at the water/air interface, the decrease in trans conformations is more rapid and remains almost unchanged from the middle till the end of the chain. At the water/DCE interface, the decrease is gradual and almost linear. The usual odd–even effect is observed and is most prominent for the water/air interface, with the odd dihedral numbers presenting a smaller percentage of trans conformations.

The percentage of trans conformations for the hexadecyltrimethylammonium chloride tails is very similar to the values obtained by Tarek et al.<sup>59</sup> with a tetradecyltrimethylammonium bromide monolayer. Böcker et al.<sup>55</sup>

obtained an average value of 81% of trans conformations for all the 17 hexadecyltrimethylammonium dihedrals. We obtained  $69 \pm 22\%$ . The large fluctuation is due to the large difference between the values of the dihedrals of the heads (mainly cis conformations) and the dihedrals of the tails.

The higher percentage of trans conformations in the CTA chain for the water/DCE interface also suggests a higher value for the average distance from the headgroup to the terminal methyl group for this interface, as can be seen in Figure 12. This distance distribution is broad at both interfaces, and most molecules have a distance that is less than the maximum probability value. A small relative maximum exists near 20 Å, corresponding to the distance of a CTA ion in the gas phase with all the tail dihedral angles in the trans conformation.

Several order parameters can be obtained by the following tensor:<sup>16</sup>

$$S_{ij} = 1/2 \langle 3 \cos \theta_i \cos \theta_j - \delta_{ij} \rangle \quad (5)$$

where  $\theta_i$  is the angle between the  $i$ th molecular axis and the monolayer normal ( $z$  axis). The order parameter is a

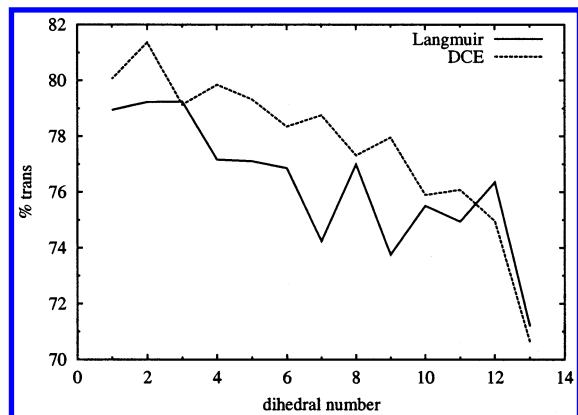


**Figure 11.** Percentage of trans conformations in the CTA hydrocarbon chains as a function of the dihedral number. On the left-hand side, we found the water lamella, and on the right the DCE lamella.

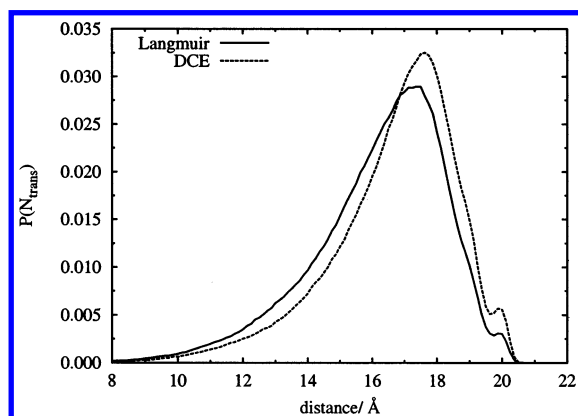


**Figure 12.** Average head to tail distance distribution.

measure of the deviation of the surfactant molecules from the monolayer normal. For each  $\text{CH}_2$  unit, we can define the  $z$  axis as the vector from the  $C_{n-1}$  to the  $C_{n+1}$  unit; the  $y$  axis is the vector in the plane of these two units and is perpendicular to the  $z$  axis; the  $x$  axis is perpendicular to the  $y$  and  $z$  axes.

The chain order parameter is usually defined as

$$S_{zz} = 1/2 \langle 3 \cos \theta_i \cos \theta_j - 1 \rangle \quad (6)$$

and is related to the local order of the long molecular axis. The experimentally observed deuterium order parameter can be obtained using the following equation:

$$S_{CD} = 2/3 S_{xx} + 1/3 S_{yy} \quad (7)$$

The values that we have obtained for the chain order parameter and for the deuterium order parameter are summarized in Figures 13 and 14, respectively. These values are in good agreement with the experimental values found for lipids chains<sup>75</sup> or values obtained by computer simulation for a dodecyl sulfate monolayer<sup>20</sup> or for phosphatidylcholine monolayers.<sup>19</sup> The values obtained for the Langmuir interface are always smaller than the values obtained for the water/DCE interface. Since a completely randomly oriented alkyl chain presents an order parameter of zero, this means that the orientation disorder is higher at the Langmuir interface. For both interfaces, the randomness in the orientation increases from the head to the tail.

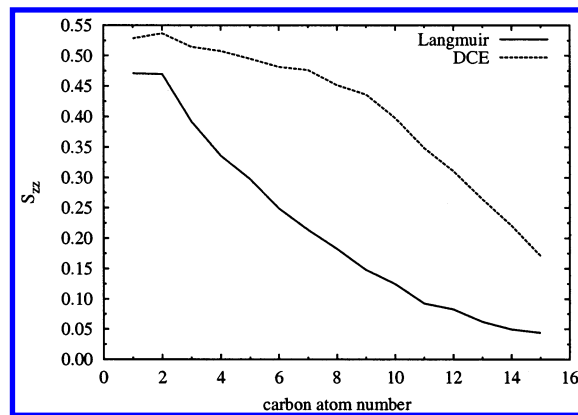


**Figure 13.** Average chain order parameter as a function of methyl number. The water lamella is located on the left-hand side, and the oil lamella on the right.

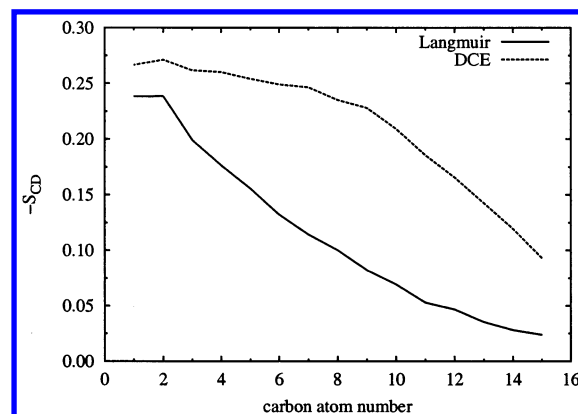


**Figure 14.** Average deuterium order parameter as a function of methyl number. The water lamella is located on the left-hand side, and the oil lamella on the right.

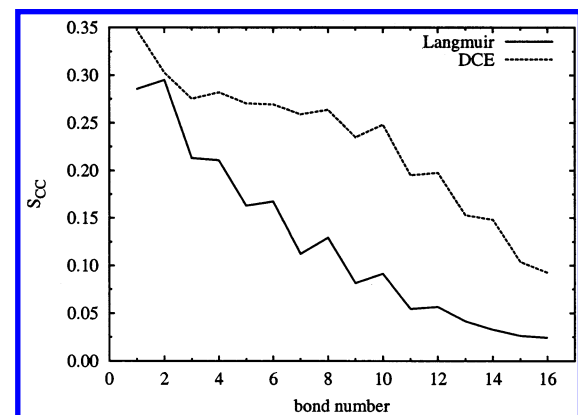


**Figure 15.** Average bond order parameter as a function of methyl number. The water lamella is located on the left-hand side, and the oil lamella on the right.

The bond order parameter is defined using the bond vector as the molecular axis. In Figure 15, the bond order parameter is displayed as a function of the methyl number, for each interface. As shown elsewhere,<sup>15</sup> the bond order parameter is a measure of the average inclination of the bond axes with respect to the monolayer normal. This property shows that the interface type can have a clear influence on the behavior of the CTA tails. For the water/air interface, the bond order parameters of all CTA tail bonds are always smaller than those for the water/DCE interface. The evolution of the bond order parameter as one goes from water to the DCE lamella is different. The decrease at the water/DCE interface is smaller than the one for the water/air interface, and a plateau exists till

(75) Sheng, Q.; Shulten, K.; Pidgeon, C. *J. Phys. Chem.* **1995**, *99*, 11018.



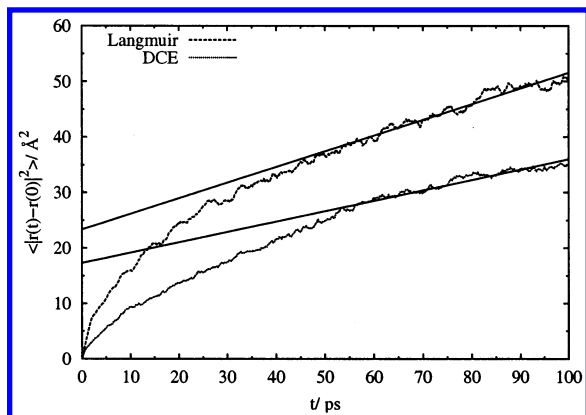


**Figure 16.** Mean square displacement of the terminal methyl group for both interfaces. A fit was made with the last 50 ps values.

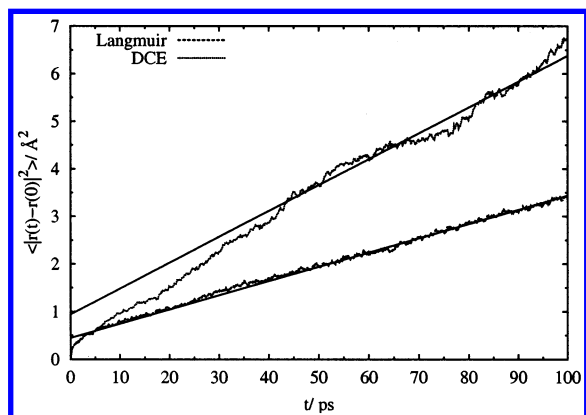


**Figure 17.** Mean square displacement of the nitrogen atom for both interfaces. A fit was made with the last 50 ps values.

the middle of the chain for the water/DCE interface. This shows that the CTA tails at the water/DCE interface are more strongly bent from the middle till the end.

In Figure 16, the in-plane mean square displacement for the terminal methyl group of the CTA chains for both interfaces is displayed. We can see that the presence of the liquid DCE phase leads to a smaller mean square displacement. This is expected since the presence of a condensed phase decreases the diffusion capability of the CTA atoms. On the other hand, and this is a rather strange behavior as an inversion occurs, the nitrogen atom presents a greater mobility at the DCE interface (cf. Figure 17).

If the motion in the monolayer plane were diffusive, the in-plane mean square displacement would obey the Einstein relation<sup>67</sup> for two dimensions (valid for long times):

$$\langle |r_j(t) - r_j(0)|^2 \rangle = 4Dt \quad (8)$$

and the diffusion coefficient parallel to the interface could be determined:

$$D = \lim_{t \rightarrow \infty} \frac{1}{4t} \langle |r_j(t) - r_j(0)|^2 \rangle \quad (9)$$

where  $r_j(t)$  is the particle position at time  $t$ . Using this relation to calculate the diffusion constant  $D$ , we find a value of  $7.05 \times 10^{-6} \text{ cm}^2 \text{ s}^{-1}$  for the diffusion of the terminal methyl group at the water/air interface and a value of  $4.68 \times 10^{-6} \text{ cm}^2 \text{ s}^{-1}$  for the water/DCE interface. These values seem quite reasonable since they are between 2.5 and 3.5 times greater than the values obtained by Tarek

et al. for the lateral diffusion of the tetradecyltrimethylammonium's mass center and it is natural that the terminal methyl group can move more freely than the large tetradecyltrimethylammonium ion.

#### 4. Summary and Conclusions

In the present study, we report a molecular dynamics simulation study of a hexadecyltrimethylammonium chloride monolayer between the water/air and water/DCE interfaces. Both the collective and individual properties of the CTA ions are studied, and a comparison is made in order to try to understand the influence of the bulk DCE lamella on the static and dynamic microscopic properties of the monolayer. Our results are in good agreement with available experimental and simulation data.

A diffusive electrical double layer was found, formed on one side by a diffusive negative layer of chloride ions and on the other by a diffusive positively charged layer formed by the CTA heads. The chloride ions do not totally neutralize the positive charge of the CTA heads, and an appropriate orientation of the water dipoles accounts for this deficiency. We also notice that an increase in the concentration of the DCE molecules exists, inside the CTA chain where they start to feel the influence of the diffuse electrical double layer.

Without a DCE lamella, the CTA tails are more folded, and the addition of the DCE bulk layer helps to stabilize the trans conformations of the dihedral angles in the CTA chains. For this reason, the CTA head to tail distance is larger at the water/DCE interface.

When analyzing the position probability distribution of the headgroup, we found that the distribution is broader when the monolayer is adsorbed at the water/DCE interface.

When changing the interface type, the tilt angle distribution of the CTA monolayer also changes. When we add the DCE molecules to the interface, the CTA chains are more aligned with the interface normal. For the water/air interface, the tilt angle distribution is sharper and has the maximum probability near  $20^\circ$  with an average of  $27^\circ$ , while for the water/DCE interface the maximum probability is located near  $40^\circ$  and the average is also  $40^\circ$ . For the water/DCE interface, there are no CTA chains which are normal to the interface, while for the water/air interface there are some chains (a very small percentage) that the tail penetrates more than the respective head.

The average number of trans conformations per chain is similar at both interfaces with a maximum probability at 12 trans conformations. Nevertheless, the percentage of dihedrals in the chains with trans conformations is greater for the water/DCE interface. For this reason, the length of the CTA ions is greater in the water/DCE interface.

The motion in the monolayer plane of the nitrogen atom and the terminal methyl group was analyzed, and it was found that the presence of a condensed phase of DCE molecules decreases the diffusion coefficient of the terminal methyl group but enhances the diffusion of the nitrogen atom.

For systems of simple liquids, the number of particles used to reproduce the properties of the thermodynamic limit is not less than 100. It is important to note that large differences exist in the collective properties of the CTA monolayer when using a rather small number of surfactants. While testing a system with only 36 CTA and 36 chloride ions, we could observe a homogeneity in the organization of the monolayer that was absent from the final 100 CTA monolayer. This is caused by the use of



periodic boundary conditions on systems with small size. We could also see on the production system some domain formation caused by the existence of canyonlike structures with dimensions of the order of half the box size. These structures are caused by the tilting of the CTA ions with a difference of about  $180^\circ$  in the azimuth orientation. In this situation, a V-shaped structure forms and when replicated in space originates the canyon structures.

Penfold et al.<sup>7</sup> pointed out that a large number of surfactant molecules should be included in the simulations because of the reduction in surface tension, the corresponding increase in the thermal fluctuation of the adsorbed monolayer, and the consequent possibility of modification in the conformations of the monolayer.

There is not much information about the behavior of monolayers at liquid/liquid interfaces, namely, information at a microscopic level that can be used to correlate

composition, structure, and dynamics. With this work, we contribute to this understanding. A still open question is about the factors that influence the behavior of the monolayers at liquid/liquid interfaces. Is it the dielectrical constant, the hydrophobicity, or the degree of penetration of the oil in the monolayer? This question is currently being addressed at our laboratory.

**Acknowledgment.** Daniel J. V. A. dos Santos thanks the *Programa PRAXIS XXI* for a doctoral scholarship (BD/15576/98). It is also a pleasure to thank Professor Natália Cordeiro for stimulating discussions. Finally, I am deeply in debt to Dr. Elsa Henriques for the manipulation of the Quanta computer program.

LA026448Q